Picky Eaters: Optimisation of a non-opsonic phagocytosis assay testing monocyte uptake of *Plasmodium falciparum* infected red blood cells

Niamh O'Sullivan

02/08/2024

Minor Research Profile, MSc. Infection & Immunity

Student Number: 2722429

Daily supervisor: Lara Bardkte, MSc.

Department of Infectious Diseases, Pulmonology and Intensive Care Medicine, Charité, Berlin, Germany

Supervisor Host Institute: Prof. Dr. Florian Kurth

Department of Infectious Diseases, Pulmonology and Intensive Care Medicine, Charité, Berlin, Germany

Examiner: Prof. Dr. Lodewijk Tielens

Department Biomolecular Health Sciences, Faculty of Veterinary Medicine, Utrecht University, Utrecht, Netherlands

Abstract

Despite efforts to improve prevention and reduce transmission, malaria remains one of the largest contributors to mortality across the World Health Organisation (WHO) African region. Protection from severe disease offered by adaptive immune memory has been well established, while the contribution of innate immune memory in malaria has not been entirely defined. One proposed mechanism suggests improved specificity and efficiency of phagocytosis by monocytes upon restimulation. We set out to develop a non-opsonic phagocytosis assay using isolated schizonts from a *P. falciparum in vitro* culture, labelled with green fluorescent protein (GFP). We stained all red blood cells (RBCs) with CellTrace dye and measured GFP+CellTrace+ monocytes, indicating phagocytosis of infected RBCs (iRBCs). We found that we could use full, thawed peripheral blood mononuclear cells (PBMCs) to measure monocyte phagocytosis and identified a population of GFP-CellTrace+ monocytes. Further optimisation steps are required to understand the cell types which comprise this population before testing patient samples.

Layman's Summary

Malaria is a parasitic infection responsible for hundreds of thousands of deaths each year. The parasites are spread by the female mosquito of the *Anopheles* species. They are passed to humans when the mosquito bites skin, injecting parasites into the bloodstream. There are several known species of parasite but one that causes many cases of infection is *Plasmodium falciparum*. The parasites first infect the liver, followed by a blood stage where parasites invade healthy RBCs. Inside the RBCs, the parasite replicates and causes cells to burst, after which they re-invade new RBCs.

Malaria infection can cause minimal or no symptoms, but it can also develop into severe disease and cause death. Studies have shown that people who have had malaria infection may experience an altered immune response if they are infected again, which can protect them from severe infection. Cases of malaria that cause little or no symptoms occur in individuals who have had infection before. This may be due to immune memory.

The immune system is divided into two arms. The adaptive immune system involves, for example, the production of antibodies, protecting an individual from infection such as, after vaccination, and has been well studied in malaria. The innate system is responsible for rapid, less specific responses. In the context of malaria, less is known about the innate immune system and innate memory.

One important mechanism of the innate immune system that can defend the host from severe infection is phagocytosis. During phagocytosis, immune cells engulf and destroy the micro-organism causing infection. Multiple different immune cells can perform phagocytosis, and one example includes monocytes.

We aimed to study how phagocytosis in malaria may be different between individuals who have experienced malaria before, compared to those who have not. A study set up at Charité University Hospital includes patient groups from Gabon, where malaria is prevalent, and travellers returning to Berlin, where it is not. Therefore, we can use these cohorts to study whether the efficiency of monocytes phagocytosing *P. falciparum*-iRBCs changes in individuals who have and have not had malaria previously, due to the development of innate memory.

We set up an experiment using isolated RBCs infected with mature stage *P. falciparum* parasites labelled with a fluorescent tag, GFP. Considering that a small portion of isolated RBCs were not infected, we stained the total RBC population with a second fluorescent dye, CellTrace. We

isolated monocytes from healthy donor blood and combined the monocytes with RBCs at different proportions. After storing for two or four hours at 37°C, we removed all RBCs which had not been phagocytosed and measured the population of monocytes which were fluorescent for both GFP and CellTrace. Monocytes stained with both dyes should contain one or more iRBCs. Using this double-staining strategy, we could distinguish whether monocytes had phagocytosed iRBCs or uninfected RBCs (uRBCs).

We found that a large proportion of monocytes were positive for CellTrace but not GFP. Further optimisation steps are required to understand the cells which comprise this population before this experiment can be used to test phagocytosis by patient monocytes.

Table of Contents

Abbreviations

BCG	Bacillus Calmette–Guérin
CD	Cluster of differentiation
CERMEL	Centre de Recherches Médicales de Lambaréné
cRPMI	Culture RPMI medium
CTFR	CellTrace Far Red
CTV	CellTrace Violet
DC	Dendritic cell
DMSO	Dimethyl sulfoxide
EDTA	Ethylenediaminetetraacetic acid
EV	Extracellular vesicle
FBS	Fetal bovine serum
GFP	Green Fluorescent Protein
iRBC	Infected red blood cell
MACS	Magnetic isolated cell sorting
MOI	Multiplicity of infection
RBC	Red blood cell
NK	Natural killer cell
PBMC	Peripheral blood mononuclear cells
PBS	Dulbecco's phosphate buffer saline
RPMI	RPMI 1640 medium
RT	Room temperature
uRBC	Uninfected red blood cell
WHO	World Health Organization

List of Tables

List of Figures

Introduction

At least 249 million cases of malaria were reported in 2022, as published by the 2023 WHO World malaria report [1]. Malaria is caused by protozoans of the genus *Plasmodium*, of which there are five known species that commonly infect humans [1, 2]. 95% of global malaria cases occur in the WHO African region where *P. falciparum* is the most prominent species [1]. While significant efforts have been made to reduce case numbers, progress has begun to plateau. This is likely due to the emergence of resistance to artemisinin-based combination therapies as well as obstacles in the rollout of prophylactic measures for healthcare systems, such as those presented by the COVID-19 pandemic [1, 3].

Malaria can result in a wide range of clinical symptoms – from asymptomatic to mild or severe disease that can ultimately lead to death [1, 2, 3]. It has been proposed that differences in disease severity and clinical presentation of malaria may depend on whether the individual has experienced the pathogen before, particularly early in life, likely when raised in an endemic setting – a state known as semi-immunity [4, 5, 6, 7].

Until recent decades, immunological memory has been considered a characteristic unique to the adaptive immune system [8, 9]. This paradigm has now shifted and innate immune cells exposed to a pathogen have been demonstrated to possibly provide enhanced protection upon subsequent exposure of the individual to the same, or different pathogen, otherwise known as innate memory [8, 9]. During a primary challenge, immune cells exposed to the pathogen undergo metabolic and epigenetic reprogramming. These adjustments can induce altered immune responses in a range of immune cells, should a secondary challenge occur by the same or different pathogen [8, 9, 10]. This was first studied following Bacillus Calmette–Guérin (BCG) vaccination whereby individuals who received the vaccine were later protected from unrelated pathogens demonstrated by increased production of pro-inflammatory cytokines [9, 11, 12]. In malaria, this has also been proposed to take place [6, 7, 13, 14].

The innate immune system protects its host from malaria via a number of mechanisms that aim to prevent invasion of parasites into host cells or destroy those cells that have been infected [13, 14]. The role of the adaptive immune response in malaria has been extensively studied, although several innate responses have not been entirely defined. At the liver stage, sporozoites that are injected into the host during the blood meal of the female *Anopheles* mosquito, target hepatocytes [14]. Sporozoites which have not yet reached the liver, can be targeted by innate cells such as dendritic cells (DCs), triggering the production of proinflammatory cytokines and

recruiting effector cells such as natural killer cells (NKs) to the site of infection [16]. During lysis of an invaded hepatocyte, free merozoites are released and the blood stage of infection begins. At this stage, host RBCs become infected and clinical symptoms can develop [13]. Monocytes and macrophages play an important role in the destruction of iRBC via phagocytosis [4, 17, 18]. *Plasmodium spp.* has developed a number of mechanisms by which it can evade recognition by the immune response such as by sequestration in endothelial tissue, enabling the parasite to avoid recognition and removal by circulating phagocytes [13, 19].

It has been suggested that innate memory may change the response of monocytes that can control *Plasmodium spp.* infection more effectively during repeat infections, when compared to individuals experiencing infection for the first time [4, 7, 20, 21]. For example, models of controlled human malaria infection have demonstrated a suppression in the production of inflammatory cytokines during acute infection which afterwards increases and promotes an enhanced immune response should repeat infection occur [21]. These inflammatory cytokines may play an important role in recruiting phagocytes to the site of infection and hence influence the efficiency of phagocytosis. Understanding the impact of immune memory on the specificity and efficiency of iRBC phagocytosis compared to uRBCs will provide insight into the protection offered by different states of immunity to malaria. The specificity of iRBC uptake is an important consideration, particularly in the context of malaria anaemia, a frequent cause of mortality especially in children and pregnant women [22]. One important determinant of severe malaria anaemia is the loss of uRBCs in excess of iRBC loss, which has also been investigated in phagocytosis [23, 24]. Improved specificity of phagocytosis would increase efficiency and hence reduce uRBC loss. It is therefore relevant to investigate the possibility of improved phagocytosis specificity and efficiency across different immune states in innate memory.

To this extent, patients with different levels of previous exposure to malaria and therefore varying levels of semi-immunity were recruited in the scope of the DEMIT study. DEMIT is a multi-centre study at Charité University Hospital (Berlin) and Centre de Recherches Médicales de Lambaréné (CERMEL) (Gabon), recruiting semi-immune patients from a malaria endemic area as well as returning travellers with no or waning semi-immunity. Cohorts of naïve and semi-immune patients include asymptomatic, symptomatic and severe cases, offering vast opportunity to study differences across various levels of disease severity.

We set out to optimise an assay which could measure non-opsonic phagocytosis of iRBC and uRBCs by monocytes, allowing us to compare the specificity and efficiency of phagocytosis across individuals of different immunity. We developed the assay using schizonts isolated from

an *in vitro* culture of *P. falciparum* 3D7 labelled with GFP. We found that we could measure activity of monocytes from full, frozen-thawed PBMCs and identified a population of monocytes which became GFP-CellTrace+. Further optimisation of this assay is required before phagocytosis of patient monocytes can be tested in order to determine the specificity and efficiency of phagocytosis across naïve and semi-immune individuals.

Materials

Parasite strain

The strain *P. falciparum* 3D7 labelled with GFP was kindly gifted by Professor Alex Maier of ANU, Canberra.

Table 1. *Materials used*

	Manufacturer
Tissue culture flask 50 mL, 25 cm^3, blue vented cap	Falcon
Tissue culture plate, 96-well, U-bottom	Falcon
Trans-well plate 6.5mm with 0.4 μm pore membrane inserts	Corning
Quadro-MACS separator	Miltenyi
LS Columns	Miltenyi
MojoSort Pan Monocyte isolation kit	Biolegend
VersaComp Antibody Capture bead kit	Beckman Coulter
SafeSeal Tips Professional	Biozym

Table 2. *Buffers used*

	Composition
MojoSort Buffer	2.5% Albumax II, 10 mM Ethylenediaminetetraacetic acid (EDTA), Dulbecco's phosphate buffer saline (DPBS)
Monocyte Medium	RPMI 1640 medium (RPMI), 10% FCS, 1% Penicillin-Streptomycin, 1X MEM NEAA, 25 mM HEPES, 1X GlutaMax
Culture RPMI medium (cRPMI)	RPMI, 0.5% Albumax II, 25 mg/L gentamicin, 25 mM HEPES, 1X GlutaMax, 100 uM Hypoxanthine in 1M NaOH
ACK lysis buffer (in-house)	0.15 M NH_4Cl, 10 mM $KHCO_3$, 0.1 M Na_2-EDTA, pure water
FACS buffer	DPBS, 2% heat-inactivated fetal bovine serum (FBS), 2 mM EDTA
Freezing Media A	RPMI, 40% heat-inactivated FBS
Freezing Media B	80% heat-inactivated FBS, 20% Dimethyl sulfoxide (DMSO)
Thawing Media	1:10,000 Pierce Universal Nuclease for Cell Lysis, 2% FBS, RPMI

Table 3. *Chemicals and solutions used*

	Manufacturer
RPMI 1640 Medium (-Glutamine)	Gibco
PDBS	Gibco
D-Sorbitol	Sigma
Pancoll (1.077 g/mL)	PanBiotech
Percoll (1.13 g/mL)	Sigma
Pure water	Fresenius Kabi
Albumax II (Lot. 2814240)	Gibco
Fresh erythrocyte concentrate	Gifted (Department of Parasitology, Humboldt University)
FBS	Sigma
Gentamicin (50 mg/mL)	Gibco
HEPES Buffer solution	Gibco
GlutaMax (100X)	Gibco
Sodium hydroxide	ThermoFisher
Hypoxanthine	Sigma
AccuStain Giemsa	Sigma
PBS tablets	ThermoFisher
RBC lysis buffer (x10) (commercial)	Biolegend
EDTA	Sigma
NH_4Cl	Merck
$KHCO_3$	Sigma
Na_4EDTA	Sigma
DMSO	Sigma
MEM Non-Essential Amino Acids (100X)	Gibco
Pierce Universal Nuclease for Cell Lysis	ThermoScientific
Penicillin-Streptamicin mix (10,0000 U Penicillin + 10 mg Streptamicin/mL)	Bio & Sell
WR (20 mM)	Gifted (Department of Parasitology, Humboldt University)

Table 4. *Equipment used*

	Manufacturer
Centrifuge	Eppendorf 5894 R
Flow cytometer	Beckman Coulter Cytoflex LX
Incubator	Binder
Microscope	Echo Revolve
Heatblock	Eppendorf Thermomixer Comfort

Table 5. *Antibodies and dyes used*

	Manufacturer	Clone	Fluorescence	Dilution
Anti-CD14	Biolegend	M5E2	PE-Cyanine7	1:50
Anti-CD16	Biolegend	3G8	Brilliant Violet 605	1:50
Anti-HLA-DR	Biolegend	L243	Brilliant Violet 785	1:50
Anti-CD3	Biolegend	UCHT1	Brilliant Violet 421	1:50
Anti-CD19	Biolegend	HIB19	Brilliant Violet 785	1:50
Anti-CD235a (Glycophorin A)	Biolegend	HI264	PE	1:100
Human TruStain FcX	Biolegend			1:50
Live/Dead Fixable Blue Dead Cell stain kit	ThermoFisher			1:500
ZombieRed Fixable Viability kit (Lot. B407223)	Biolegend			1:500
CellTrace Far Red Cell Proliferation kit	ThermoFisher			1:2000
CellTrace Violet Cell Proliferation kit	Biolegend			1:1000
Hoechst 33342 Nucleic Acid stain (Lot. YB3830692)	ThermoScientific		DAPI	1:1000

Methods

1. *Plasmodium falciparum* culture

P. falciparum was maintained *in vitro* using 75 cm^3 culture flasks according to the candle-jar method originally established by Trager and Jensen [25]. The strain *P. falciparum* 3D7 labelled with GFP was kindly gifted by Professor Alex Maier of the Division of Biomedical Sciences and Biochemistry at ANU, Canberra. Cultures were maintained at a haematocrit of approximately 5% and stored in an incubator at 37°C. The candle-jar method involves storing culture flasks with breathable lids of *P. falciparum* culture in a sealed plastic box containing a candle and small container of water. Each time the box is closed, the candle is lit and once shut, the flame will extinguish to create the optimum gaseous conditions required to maintain *P. falciparum* cultures, consisting of estimated 17% O_2, 3% CO_2, and 80% N_2 [25]. Culture parasitaemia was maintained between 1-3% depending on use. Parasitaemia was confirmed with blood smears stained with Giemsa counted on the Echo Revolve microscope. Smears were performed using a droplet of approximately 2 μL culture, fixed with methanol and left to dry. Slides were stained in 20% Giemsa in pure water for approximately 10 min and excess stain was removed with pure water. Slides were left to dry before visualising under the microscope using the x100 objective and immersion oil. Sub-culturing was completed every two to three days, using fresh human erythrocyte concentrate (O+ blood group) which were used for no longer than four weeks, and cRPMI. cRPMI was prepared as described and filter sterilised. To test the DNA content and GFP expression of *P. falciparum* culture, a culture of mixed stage parasites at approximately 5% parasitaemia was stained with Hoechst 33342 Nucleic Acid stain in PBS and incubated for 30 min in the dark at RT. After staining, the culture was centrifuged for 5 min at 300 xg and the pellet was resuspended in FACS buffer, prepared as described, to measure on a flow cytometer.

2. Culture synchronisation

Synchronisation of cultures containing at least 5% ring-stage parasites was complete before each experiment using D-sorbitol (5%) prepared in MilliQ water and filter sterilised. To synchronise, cultures were centrifuged for 5 min at 400 xg. The RBC pellet was resuspended in x10 the volume of 5% D-sorbitol and incubated for 10 min at 37°C. The pellet was then washed twice with cRPMI by centrifuging at 300 xg for 5 min at RT. The RBC pellet was then resuspended in cRPMI at culture conditions of 5% haematocrit and incubated for a further 32 to 36 hours

before schizont isolation. Late stage schizonts were isolated for each experiment using either Percoll or magnetic isolated cell sorting (MACS) isolation.

3.   Schizont isolation

Schizont isolation was performed using Percoll or MACS isolation. To isolate with Percoll, 5 mL cultures containing at least 5% late trophozoites or schizonts were layered over 63% or 70% Percoll, prepared in x10 PBS and MilliQ water, and centrifuged at 5000 xg for 10 min without brakes. Schizonts separated on the basis of density were isolated from the suspended layer between Percoll and culture medium with a Pasteur pipette. Schizonts were washed twice before use with cRPMI by centrifuging at 300 xg for 5 min at RT. Isolation with MACS was completed using 7 mL cultures of at least 6-10% schizonts. LS columns were calibrated with PBS on the QuadroMACS separator and cultures were added to separate iRBCs and uRBCs on the basis of magnetic isolation. PBS with 10 mM EDTA was used to flush schizonts from the LS column. Schizonts were washed with cRPMI before use by centrifuging for 5 min at 400 xg. Schizont purity was determined using blood smears stained with Giemsa by counting the proportion of schizont iRBC expressed as a percentage of the total RBC population. Purity of schizonts varied between 60-75% between experiments.

4. PBMC isolation, seeding and thawing

PBMC isolation was based on previously established methods [26]. Blood filters were obtained from the Centre for Transfusion Medicine, Charité. Blood filters were rinsed with PBS containing 2 mM EDTA and a maximum of 30 mL of diluted blood was layered over 20 mL Pancoll. After centrifugation for 25 min without brakes at 800 xg, the cloudy cell layer was removed with a Pasteur pipette and washed twice in PBS at 400 xg for 15 min at 4°C and afterwards at 350 xg for 15 min at 4°C. An erylysis step was carried out if the pellet remained bloody by adding 2 mL of commercial RBC lysis buffer (x10) in MilliQ water. After incubating for 5 min at RT, cells were washed at 350 xg for 10 min at 4°C and PBMCs were counted with Trypan Blue in a Neubauer chamber.

To freeze, isolated PBMCs were spun at 350 xg for 10 min at 4°C and resuspended in Freezing Media A to 1×10^7 cells/mL. Following this, an equal volume of Freezing Media B is added slowly, dropwise to final cell count of 5×10^6/mL. Aliquots of 1 mL cell suspension were stored in cryovials in CellCampers at -80°C overnight and later transferred to -150°C for long-term storage. Frozen PBMCs, were thawed using pre-warmed Thawing Media. 1 mL aliquots of PBMCs were gradually thawed in a water bath at 37°C, suspended in 10 mL Thawing Media and washed twice

at 400 xg for 5 min, resuspending each time with Thawing Media. Cells were counted, seeded at 5×10^5 cells per well in Monocyte Media and incubated for 1 or 3 hours at 37°C in a 96-well U-bottom plate. After incubation, non-adherent cells were removed by rinsing the wells twice with PBS. Alternatively, monocytes were isolated from full PBMCs using the MojoSort Pan isolation kit.

5. Monocyte isolation

Monocytes were isolated using the MojoSort Human Pan Monocyte Isolation kit by negative selection according to the manufacturer's protocol. Briefly, isolated PBMCs were suspended at 1×10^8 cells/mL in MojoSort Buffer. In a propylene tube, cells were incubated first with an Fc receptor blocking solution for 10 min at RT. A biotinylated-antibody cocktail was then added, containing antibodies against cluster of differentiation (CD) 20, CD56, CD123, CD7, CD15, CD19, CD235ab, CD57, and CD3, and incubated on ice for 15 min. Streptavidin nanobeads were then added to label all antibody-labelled cells and incubated for 15 min. Following a series of washing steps, the propylene tube was placed on a magnet whereby all labelled cells adhere to the tube and monocytes were poured out. Total cells numbers were counted before seeding for each experiment as described.

6. Phagocytosis assay

Isolated schizont-iRBCs were suspended to 1×10^7 cells/mL. Fresh erythrocyte concentrate was used as the uRBC control in each experiment. All RBCs were labelled using the CellTrace Far Red (CTFR) Cell Proliferation kit or CellTrace Violet (CTV) Cell Proliferation kit for 20 min at room temperature (RT) in the dark. Monocyte Media was added after staining to quench excess dye and cells were washed for 5 min at 300 xg. iRBCs and uRBCs were suspended in pre-warmed Monocyte Media at various multiplicity of infection (MOI) and added to previously seeded PBMCs. The MOI was calculated including iRBCs only, based on the schizont purity established following isolation. Cells were incubated for two or four hours at 37°C. After incubation, cells were immediately centrifuged at 4°C for 5 min at 500 xg to stop phagocytosis. ACK lysis buffer was prepared in MilliQ water (x10) and added to lyse all non-phagocytosed RBCs by incubating at RT for 10 min. Cells were washed twice for 5 min at 300 g, resuspended in 1:500 Live/Dead Fixable Blue Dead Cell stain kit or ZombieRed Fixable Viability kit prepared in PBS and incubated for 20 min at RT in the dark. To block Fc receptors, Human TruStain FcX was then added and cells were incubated for a further 10 min at RT in the dark. Cells were washed twice with FACS Buffer, and resuspended in an antibody cocktail containing anti-CD14, anti-CD16, anti-CD3, anti-CD19,

anti-HLA-DR, anti-CD235a prepared in FACS buffer. Cells were incubated for 30 min at 4°C in the dark. Cells were washed twice and resuspended in FACS Buffer to measure with flow cytometry. Potential leakage of the CellTrace dye from RBCs was tested using trans-well plates by seeding 5×10^5 PBMCs per well as previously described and resting for 3 hours. To the top insert of the plate, iRBCs and uRBCs were added at an MOI of 5 and incubated for 4 hours at 37°C. The inserts containing RBCs were then removed and the PBMCs were stained as per previous experiments already described.

7. Flow cytometry

Cells were acquired with the CytoFLEX LX. Compensation was performed before each experiment using VersaComp Antibody Capture Bead kit. Briefly, beads were diluted in FACS Buffer and incubated with each used antibody (1:100) as well as unstained bead and cell controls, for 30 min at 4°C in the dark. Following incubation and centrifugation at 500 xg for 5 min, beads were resuspended in FACS Buffer for measurement. For Live/Dead controls, PBMCs were incubated on a heat-block for 10 min at 56°C, combined with live cells stored on ice and stained with the respective Fixable Live/Dead kit as described previously. Compensation of GFP fluorescence was performed using a sample of isolated schizonts prepared for the experiment prior to CellTrace staining. For CellTrace compensation, a sample of uRBCs was stained with CellTrace, as described and combined with unstained RBCs.

8. Microscopy

Microscopy was performed using the Echo Revolve Microscope for both the confirmation of parasitaemia with Giemsa stained slides and for fluorescent imaging. The x100 objective and immersion oil was used to visualise slides.

9. Statistical methods

Flow cytometry data was analysed using FlowJo (version 10.10). Graphs were produced using GraphPad Prism10.

Results

1. Development of non-opsonic phagocytosis assay

Strongest GFP fluorescence signal expressed by late-stage *P. falciparum* 3D7

We set out to develop an assay that could test the non-opsonic phagocytic capacity of monocytes from patients with different states of immunity to malaria to compare differences in the efficiency and specificity of iRBC and uRBC uptake. We developed our assay using parasites from an *in vitro* culture of *P. falciparum* 3D7 labelled with GFP. We first set out to identify what stage of parasite most strongly expressed GFP fluorescence using flow cytometry. We tested cultures containing parasites at each lifecycle stage and could identify the different parasite stages based on the quantities of DNA present, stained with Hoechst 33342 Nucleic Acid stain. Here we saw that later stage parasites, containing higher quantities of DNA, also expressed more GFP (Fig. 1B). This was confirmed by measuring the signal of Hoechst and GFP expression by schizonts isolated using 63% Percoll (Fig. 1C). We therefore opted to use isolated schizonts to develop our assay.
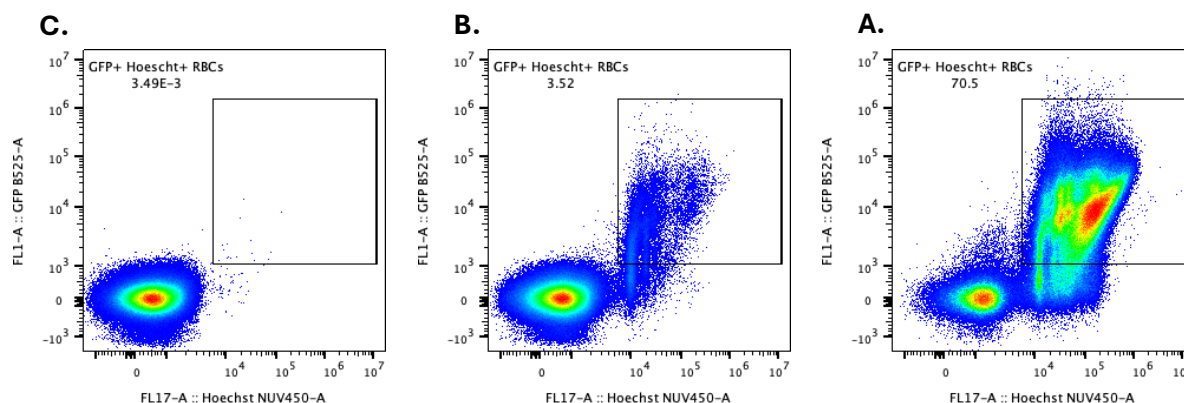

Figure 1. Late-stage parasites expressed more GFP compared to early-stage parasites.
*GFP and Hoescht signal of **(A)** uRBCs, **(B)** mixed stage* P. falciparum *culture and **(C)** isolated* P. falciparum *schizonts. Fresh RBCs as a negative control, a mixed stage* in vitro *culture of approximately 5% parasitaemia and schizonts isolated from* P. falciparum *3D7 labelled with GFP using 63% Percoll were stained with Hoechst 33342 Nucleic Acid Stain at a concentration of 1:1000 in PBS. RBCs were measured by flow cytometry and data was analysed in FlowJo 10.10. Figure is representative of one experiment.*

MACS separation isolated schizonts with the higher purity compared to Percoll

We tested two methods to isolate schizont-stage iRBCs from *in vitro P. falciparum* 3D7 culture. Using the MACS separator, we isolated schizonts on the basis of the magnetic content of hemozoin contained in late-stage schizonts (Fig. 2A). Using Percoll, we separated schizont-iRBCs on the basis of density (Fig. 2B). Preparations of 63% and 70% Percoll were trialled to optimise the isolation with the greatest proportion of schizont-stage iRBCs where isolation with 63% Percoll produced schizonts of higher purity (data not shown). We found that MACS isolation

produced a culture of higher iRBC purity with fewer extracellular parasites compared to isolation using Percoll, and for later experiments utilised MACS separation for schizont-iRBC isolation.
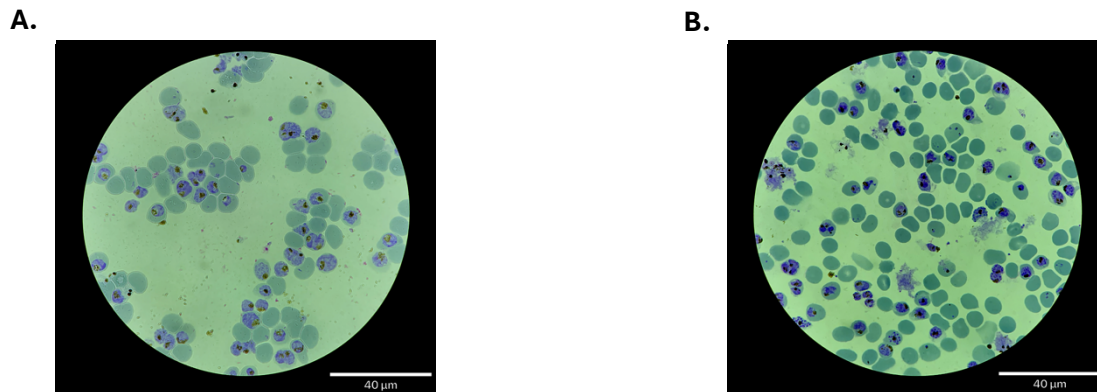
A.

B.

Figure 2. Schizont isolation using MACS separation produced iRBCs with higher purity.
Giemsa-stained smears of isolated schizonts using (A) MACS separation and, (B) Percoll at 63%. Schizont purity was calculated based on the percentage of iRBCs of the total RBC population. Images taken with the Echo Revolve microscope using the x100 objective.

MojoSort Pan Monocyte isolation resulted in high cell loss and low monocyte yield

We performed monocyte isolations using the MojoSort Pan Monocyte isolation kit. Using this kit, we identified populations of classical, intermediate and non-classical monocytes based on CD14 and CD16 expression. From full PBMCs, CD14+ and CD16+ cells were separated by negative selection by removing cells positive for antibodies CD20, CD56, CD123, CD7, CD15, CD19, CD235ab, CD57, and CD3. We found that using the MojoSort Pan monocyte isolation kit, we isolated few CD14+CD16- monocytes. We analysed cell populations from flow cytometry using FlowJo (V10.10), gating on the total PBMC population, and ruling out doublets or dead cells. Isolated monocytes were HLA-DR+, with differing expression of CD14 and CD16 (Fig. 3). We experienced high cell loss and low yield during monocyte isolation using the MojoSort kit, with a yield of between 3.4×10^5 and 5.8×10^5 monocytes, which constitutes 1.7-2.9% of total PBMCs used (approximately 2×10^7 PBMCs).
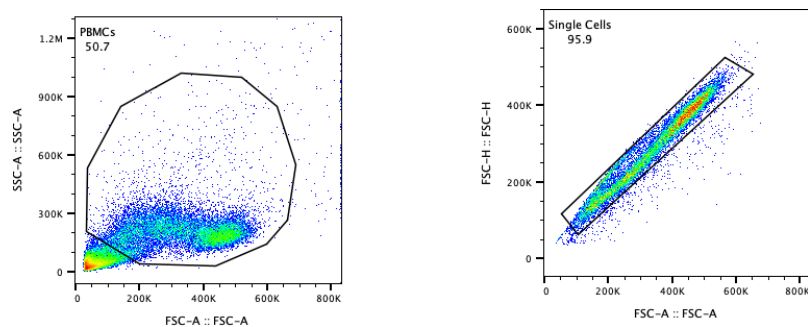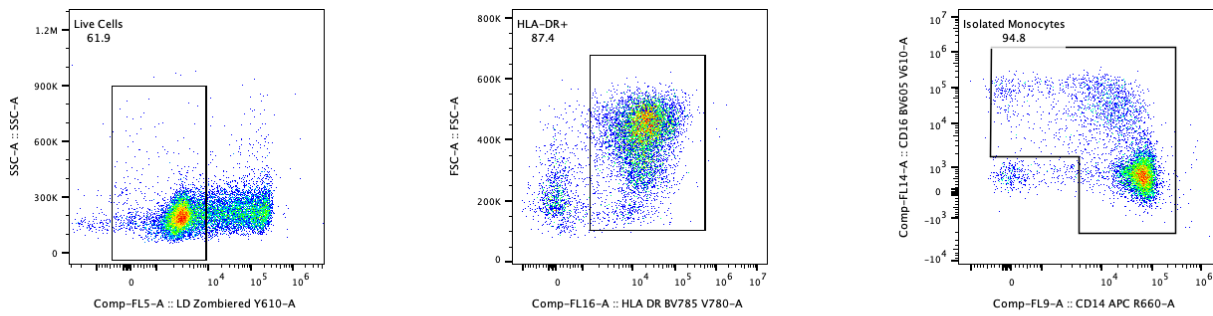
Figure 3. Monocyte gating strategy.
Monocytes were isolated from PBMCs using the MojoSort Pan Monocyte isolation kit. PBMCs were gated from the total cell population based on size and granularity, followed by single cells to exclude doublets. Live cells were separated based on Live/Dead Fixable Blue staining. Monocytes were gated on HLA-DR+ events and CD14/CD16 expression measured. Samples were measured by flow cytometry and data was analysed in FlowJo 10.10. Figure is representative of one experiment.

P. falciparum-GFP schizonts and isolated monocytes were tested for phagocytic activity

Using schizonts labelled with GFP and monocytes isolated from PBMCs, we developed our assay to test for non-opsonic phagocytosis. After performing the schizont isolation, we stained all RBCs with either CTFR or CTV, to also account for uRBCs obtained during the schizont isolation. Including both dyes allowed us to distinguish phagocytosis specifically of iRBCs compared to uRBCs, to eventually determine specificity of phagocytosis by patient monocytes. In addition, we included in our experiments, fresh RBCs from erythrocyte concentrate as a negative control.
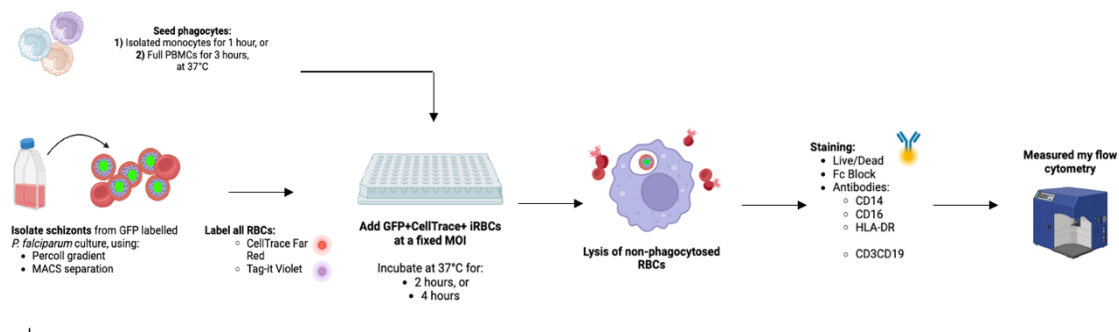

Figure 4. Graphical abstract of experimental overview.
Phagocytes were seeded for one or three hours at 37 ℃. Schizonts were isolated from in vitro *culture of* P. falciparum *3D7 labelled with GFP, using Percoll or MACS separation. iRBCs are added to phagocytes at a fixed MOI and incubated for two or four hours at 37 ℃. Non-phagocytosed RBCs are lysed and monocytes are stained. Samples are measured with flow cytometry. Made with BioRender.*

Therefore, iRBCs should be labelled with both GFP and CTFR/CTV. We added stained RBCs to seeded monocytes at a fixed MOI. After incubating at 37°C for two or four hours, we stopped phagocytosis by introducing an immediate centrifugation step at 4°C. Following this, we performed RBC lysis to lyse all RBCs that were not phagocytosed by monocytes. Afterwards, we stained for dead cells and blocked all Fc receptors . We finally stained with a panel of antibodies including anti-CD14, anti-CD16 and anti-HLA-DR. From the 96-well plate which was used to perform the experiment, we could also remove monocytes to visualise with fluorescent microscopy and validate our experiment design.

Increasing MOI does not impact GFP+CellTrace+ population

Once we developed our assay, we tested several MOI values. We performed our assay testing MOI values of 5, 10 and 20. Higher MOI values of 100 and 200 were also tested which resulted in high cell death and therefore was excluded from future experiments (data not shown). The MOI was calculated based on the number of iRBCs indicated by the schizont purity, which represents iRBCs as a proportion of the total RBC population. Phagocytosis was measured by determining the portion of GFP+CellTrace+ monocytes, which signified phagocytosis of iRBCs. We found that increasing the MOI from 5 to 20 did not greatly impact the proportions of GFP+CellTrace+ monocytes relative to the total monocyte population with 36% and 35.9% GFP+CellTrace+ population, respectively (Fig. 5).
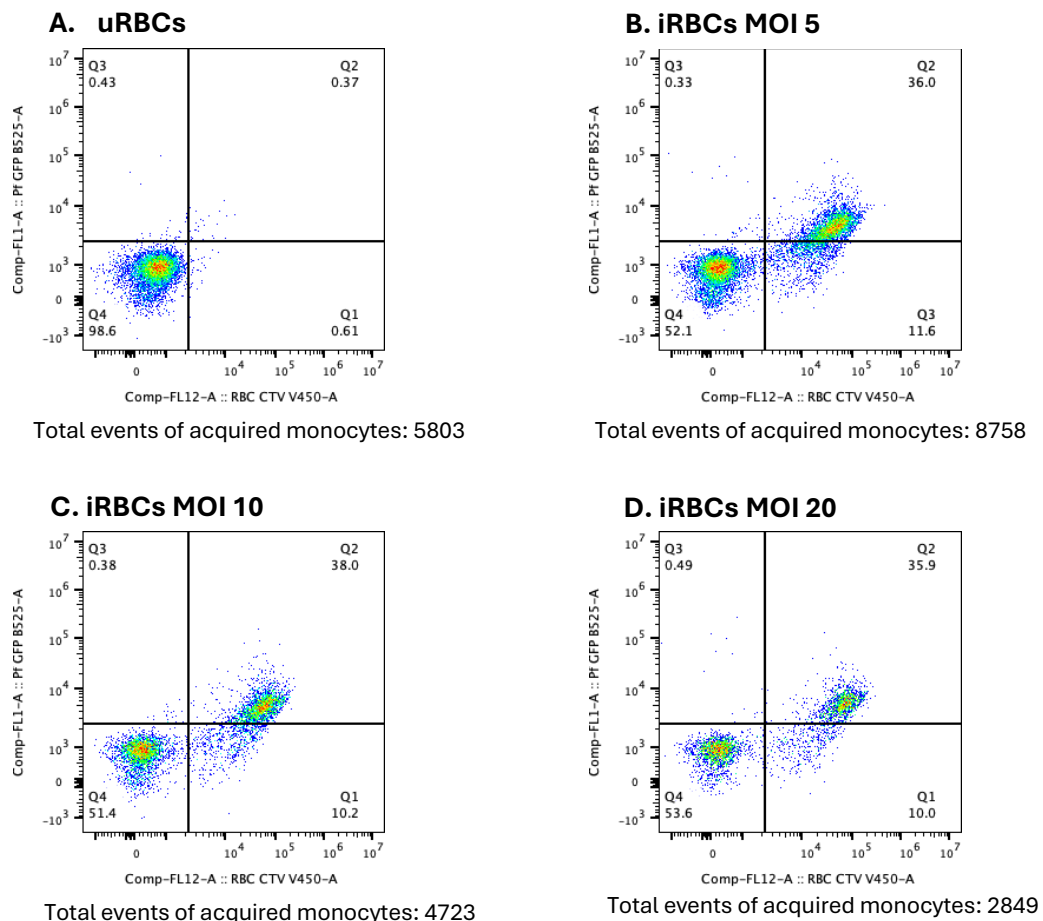

A. uRBCs

Total events of acquired monocytes: 5803

B. iRBCs MOI 5

Total events of acquired monocytes: 8758

C. iRBCs MOI 10

Total events of acquired monocytes: 4723

D. iRBCs MOI 20

Total events of acquired monocytes: 2849

Figure 5. Increasing the MOI did not greatly impact proportions of GFP+CellTrace+ monocytes.
Cells are pregated on monocytes. Proportions of GFP+CellTrace+ monocytes compared to GFP-CellTrace+ monocytes remained similar across MOI values, measured in (A) uRBCs, iRBCs at MOI of (B) 5 , (C) 10 and (D) 20. With increasing MOI, the event number decreased, indicated by the lower recorded number of monocytes and lower live cell proportions. Total RBC populations were labelled here with CTV. Samples were measured by flow cytometry and data was analysed in FlowJo 10.10. Figure is representative of one experiment.

However, with increasing MOI, the percentage of live cells slightly decreased, measured as a percentage of the population of PBMCs (47.8% of PBMC population in the uRBC control were live

cells, 16.9% iRBC at MOI of 5, 11.5% iRBC at MOI of 10, 8.94% iRBC at MOI of 20). We also recorded lower number of monocytes at higher MOI (Fig. 5). For this reason, we used an MOI of 5 in future experiments.

2. Full frozen-thawed PBMCs demonstrate similar functional activity to freshly isolated monocytes

Monocytes isolated from frozen-thawed PBMCs retain phagocytic capacity

With the established parasite stage and MOI identified, we then optimised the isolation of monocytes, our target cell population. We aimed to develop this assay for use of patient samples collected as part of the multi-centred 'DEMIT' study, performed at Charité including patients from CERMEL, Gabon. For this reason, given the transport of precious patient material is performed frozen, we aimed to optimise our assay to use frozen-thawed material. We tested isolated monocytes, using the MojoSort Pan Monocyte isolation kit, from freshly isolated PBMCs and compared their phagocytic capacity to monocytes isolated from PBMCs which had been frozen (Fig. 6).
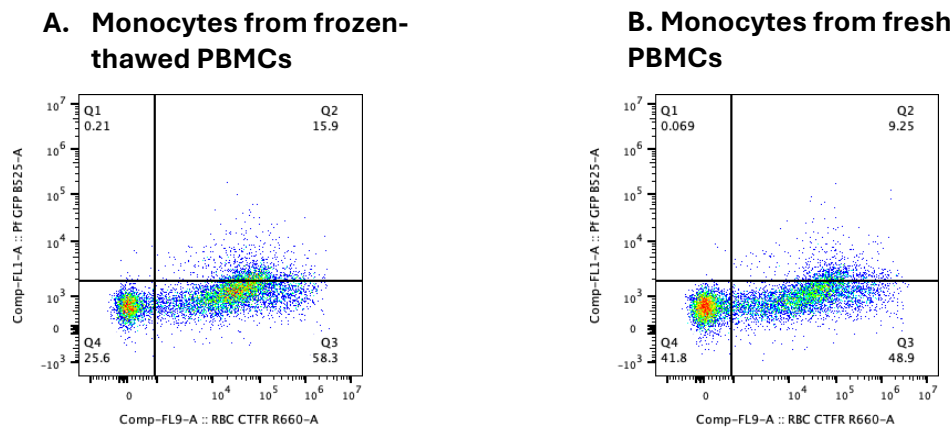
A. Monocytes from frozen-thawed PBMCs   B. Monocytes from fresh PBMCs

Figure 6. Freezing had a minimal impact on the phagocytic activity of monocytes.
Cells are pregated on monocytes. Proportions of GFP+CellTrace+ cells remain similar measured in monocytes isolated from (A) frozen-thawed PBMCs, and (B) freshly PBMCs. Pan-monocytes were isolated either from frozen-thawed PBMCs, thawed as methods describe, or from freshly isolated PBMCs. Samples were measured by flow cytometry and data was analysed in FlowJo 10.10. Figure is representative of one experiment.

We found that the percentage of GFP+CellTrace+ monocytes from frozen-thawed PBMCs was slightly greater than from freshly isolated PBMCs (15.9% compared to 9.25%). These monocytes, while coming from the same donor, were collected on different days, which may explain the increase in activity demonstrated by frozen-thawed PBMCs which we did not anticipate. From this analysis, we deduced that monocytes isolated from frozen PBMCs do demonstrate similar phagocytic activity to freshly isolated monocytes and could be utilised in future assays.

Phagocytic capacity of monocytes can be measured in full PBMCs

It has been demonstrated in literature that cells other than monocytes, included in PBMCs are important in mediating the uptake of iRBCs. As shown in the study by Crabtree et al., T cell-depleted PBMCs and isolated monocytes alone did not induce the same innate immune training, via production of cytokines such as IL-6 and TNF, when compared to full PBMCs [27]. For this reason, we sought to use full PBMCs in our assay. Additionally, we observed a high cell loss when performing monocyte isolation which we hoped to reduce, particularly when testing limited patient material. We showed that using full frozen-thawed PBMCs, a similar proportion of GFP+CellTrace+ monocytes were measured, compared to previous experiments using isolated monocytes (Fig. 7).
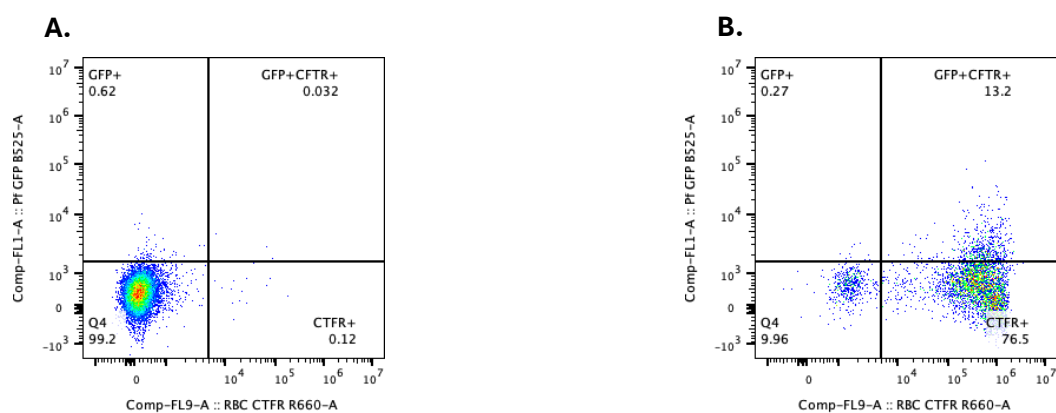

Figure 7. Full frozen-thawed PBMCs can be used to measure phagocytosis of monocytes.
Cells are pregated on monocytes. Proportions of GFP+CellTrace+ monocytes measured in (A) uRBCs and (B) full, thawed PBMC demonstrated similar activity to previously performed experiments using isolated monocytes. PBMCs were thawed as previously described. Samples were measured by flow cytometry and data was analysed in FlowJo 10.10. Figure is representative of one experiment.

PBMC rest period of three hours increases the monocyte proportion of adherent cells

Using full PBMCs in our assay allows for some form of cross-talk among B and T lymphocytes with phagocytes that can play a role in mediating uptake of iRBCs. The mechanisms of such interactions have yet to be clearly defined. However, in our assay, we were primarily interested in measuring the phagocytic capacity of monocytes. We sought to enhance the monocyte population in PBMCs by trialling longer resting periods, during which monocytes would adhere to the plate wells, and non-adherent cells such as B and T lymphocytes would be removed during a series of washing steps. In this way, the initial interactions between lymphocytes and phagocytes can take place while our read-out of monocytes may be improved. We tested resting periods of one and three hours to test what proportion of B and T lymphocytes and NK cells would be removed during washing. We found that by resting full PBMCs for three hours and washing with PBS, the remaining adherent PBMC population contained a lower proportion of CD3+ cells, CD19+ cells and CD56+ cells compared to PBMCs rested for 1 hour (Fig. 8). In the media-only

control, the population of CD3+CD19+ cells was reduced from 16.8% to 12.1% between one and three hours resting. Additionally, the population of CD56+ cells was reduced from 2.4% to 1%. The total count of monocytes did appear to reduce over time, possibly due to a small population of PBMCs that may die during this time which is increased in longer rest periods (Supplemental Fig. 1). The impact of these populations in phagocytosis by monocytes remains to be studied.
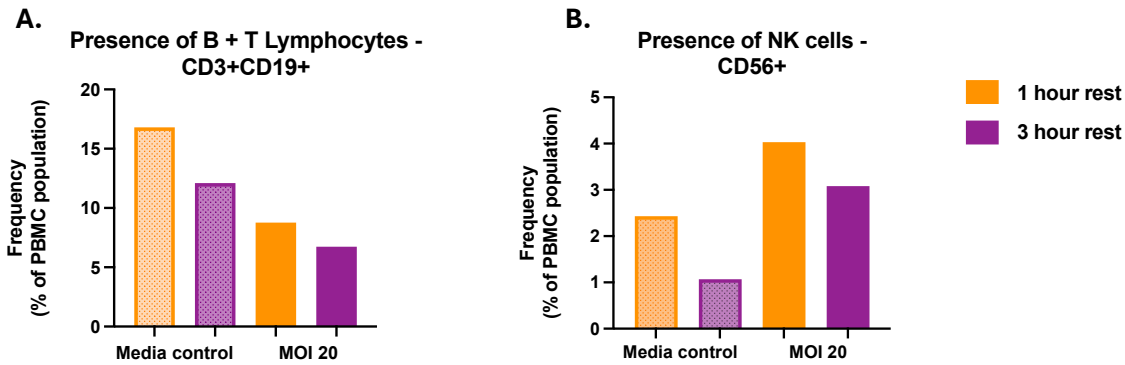

Figure 8. Resting freeze-thawed full PBMCs for three hours reduced the proportion of CD3+, CD19+ and CD56+ cells. *Populations of (A) B and T lymphocytes and (B) NK cells were measured in PBMCs which had been rested for one hour (shown in orange) or three hours (shown in purple) prior to the addition of iRBCs. Schizonts were added to monocytes at an MOI of 5 and incubated for four hours at 37ºC. Samples were measured by flow cytometry and data was analysed in FlowJo 10.10. Figure is representative of one experiment. Figure produced using GraphPad Prism 10.3.*

3. Optimisation of GFP-CellTrace+ population in PBMCs

We found that when measuring the population of CellTrace+ monocytes in our assay over a number of experiments in different conditions, a larger proportion of cells were GFP- compared to GFP+. We trialled several optimisation steps to understand whether the GFP-CellTrace+ monocyte population indeed consisted of uRBCs that were being phagocytosed or could be explained differently in our assay.

We first hypothesised that the *in vitro* culture set-up which we maintained, may be altering the surface structure of the uRBCs present in our final isolated schizont population. It is possible that the conditions created by the candle-jar method of culturing *P. falciparum in vitro*, may induce changes to either iRBCs or uRBCs that can influence phagocytosis of RBCs and possibly explain the increased proportion of GFP-CellTrace+ RBCs phagocytosed compared to GFP+ [28, 29, 30]. We therefore cultured fresh RBCs under the same culture conditions as our *P. falciparum* culture for at least one week. When we compared the 'cultured' uRBCs to fresh RBCs, which were used as controls in previous experiments, we saw minimal difference in the population of CTFR+ cells (Fig. 9). Using fresh RBCs produced a background signal of 1.23% compared to 'cultured' RBCs of 0.51%. We concluded that these culture conditions must not be responsible for the development of this population in our assay.
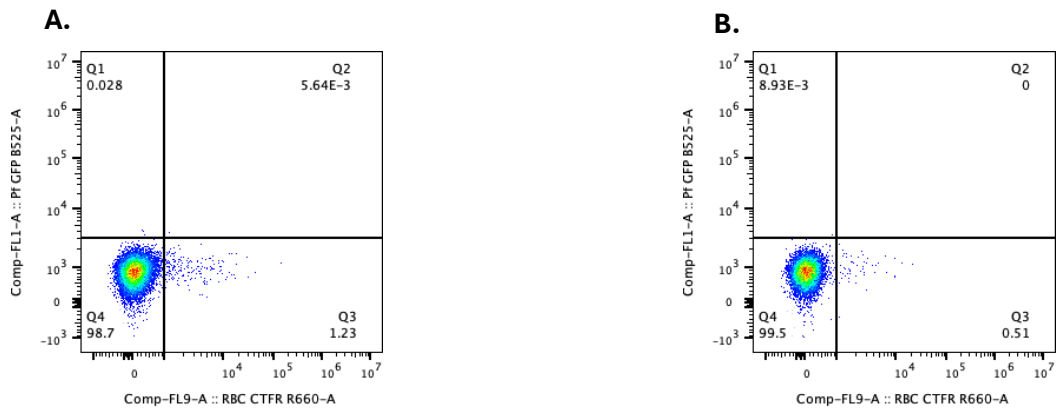
Figure 9. *In vitro* culture conditions do not appear to influence the uptake of uRBCs.
Cells are pregated on monocytes. Frequencies of GFP-CellTrace+ monocytes were compared between (A) fresh RBCs and (B) 'cultured' RBCs to assess the impact of culture conditions on the uptake of uRBCs. Samples were measured by flow cytometry and data was analysed in FlowJo 10.10. Figure is representative of one experiment.

Considering that culture conditions did not appear to induce uRBC phagocytosis alone, we then set out to test whether the CellTrace is leaking from the stained RBCs. Leaking CellTrace dye may be taken up by monocytes that are then measured in the CellTrace+ population without actually phagocytosing CellTrace+ RBCs. To test this, we used a trans-well plate, preventing direct contact of RBCs and monocytes, and therefore phagocytosis. CellTrace+ monocytes detected in this assay therefore must be as result from leaking dye. Here, we seeded PBMCs in the bottom well as previously described. To the top sections of the plates, we added RBCs stained with CellTrace. We did not measure a clear population of CellTrace+ monocytes, indicating that dye was not leaked into media by intact RBCs, or was not taken up by monocytes (Fig. 10). No clear differences were observed between iRBCs or uRBCs. In this experiment, we removed the insert containing RBCs directly after incubation and so RBC lysis was not necessary. Alternative methods of measuring leakage of CTFR should be considered.
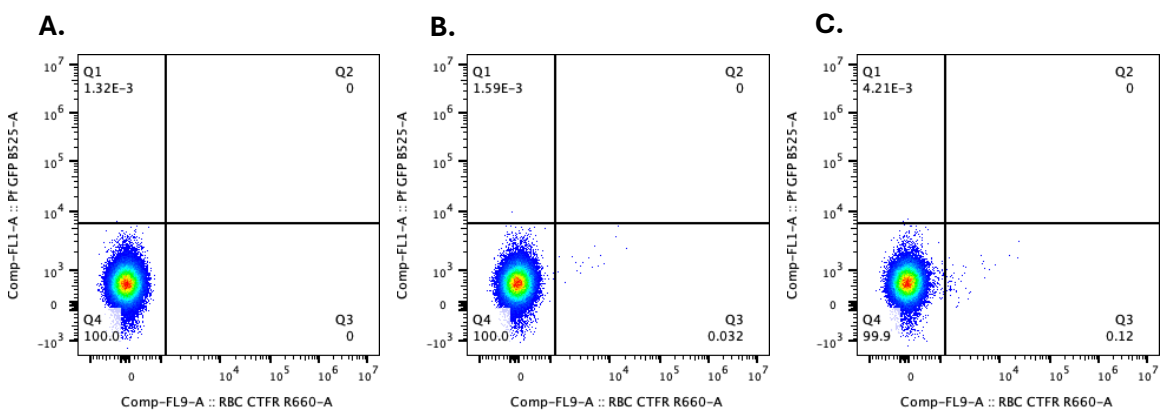

Figure 10. Intact RBCs did not leak CellTrace dye into media for monocyte uptake.
Cells are pregated on monocytes. Frequencies of GFP-CellTrace+ monocytes were compared between a (A) media only control, (B) stained iRBCs and (C) stained uRBCs to distinguish whether dye leakage may be responsible for proportions of GFP-CelLTrace+ monocytes. Schizonts were added to monocytes at an MOI of 5 and incubated for four hours at 37°C. Samples were measured by flow cytometry and data was analysed in FlowJo 10.10. Figure is representative of one experiment.

Following this, we considered whether monocytes adhering to RBCs instead of phagocytosing them, may provide an alternative explanation for the high proportion of GFP-CellTrace+ monocyte population. To test this theory, we performed an experiment whereby the incubation step of four hours was performed at 4°C to inhibit phagocytosis. We found that without phagocytosis, still 19.2% of monocytes were GFP-CellTrace+. We can see that the lack of GFP+ monocytes indicates that phagocytosis was likely indeed inhibited. We concluded from this, that monocytes adhering to RBCs might be responsible for a subset of the high proportion of GFP-CellTrace+ monocytes observed in our assay, but not all, as we constantly observe frequencies of 48-76%.
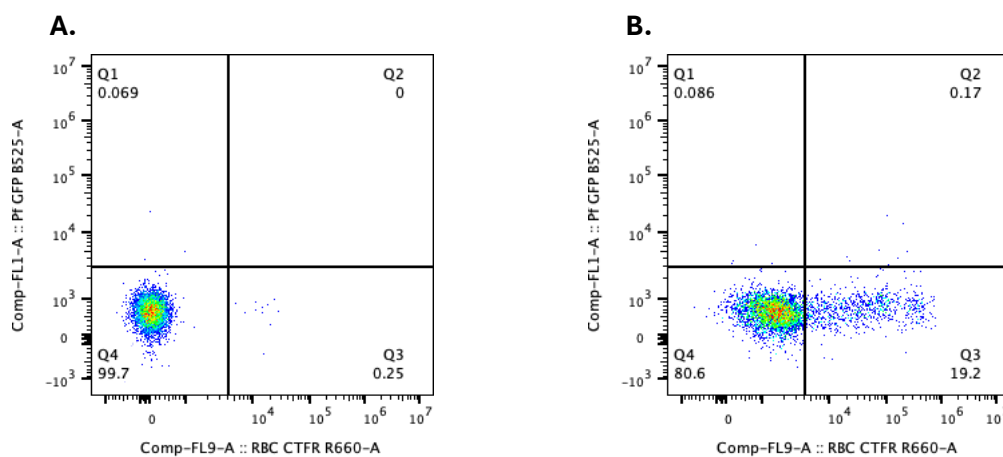

Figure 11. Adherence of uRBCs to monocytes may be responsible for a proportion of the GFP-CellTrace+ population.
Cells are pregated on monocytes. Frequencies of GFP-CellTrace+ monocytes compared between (A) uRBCs and (B) iRBCs after phagocytosis was inhibited by incubating the plate with both samples at 4°C instead of 37°C. Schizonts were added to monocytes at an MOI of 5 and incubated for four hours at 4°C. Samples were measured by flow cytometry and data was analysed in FlowJo 10.10. Figure is representative of one experiment.

As we showed that adherence of RBCs to the outer surface of monocytes may be responsible for a fraction of the GFP-CellTrace+ population, we finally considered the RBC lysis procedure of our experimental set-up. During this step, all non-phagocytosed RBCs should be lysed using a lysis buffer produced in-house, containing NH_4Cl, $KHCO_3$ and Na_4EDTA as described. We considered that if this step is insufficiently lysing these non-phagocytosed RBCs, which could be uRBCs, it may contribute to the high proportion of GFP-CellTrace+ monocytes. We tested a number of different lysis buffers including one commercially available buffer produced by Roche, and tested a variety of concentrations and volumes of the buffer produced in-house, used in previous experiments. We found that using the commercial lysis buffer compared to the in-house buffer at different volumes and concentrations, did not greatly influence the proportion of GFP-CellTrace+ monocytes (59.6% using the Roche RBC lysis buffer, 55.6% using x10 concentration of our own lysis buffer and 52.7% using x10 volume of our own lysis buffer) (Fig. 12). Using

increased volumes, which required the monocytes to be removed from the plate, resulted in a large loss in cells and caused a low event count in our final read-out (Fig. 12D).
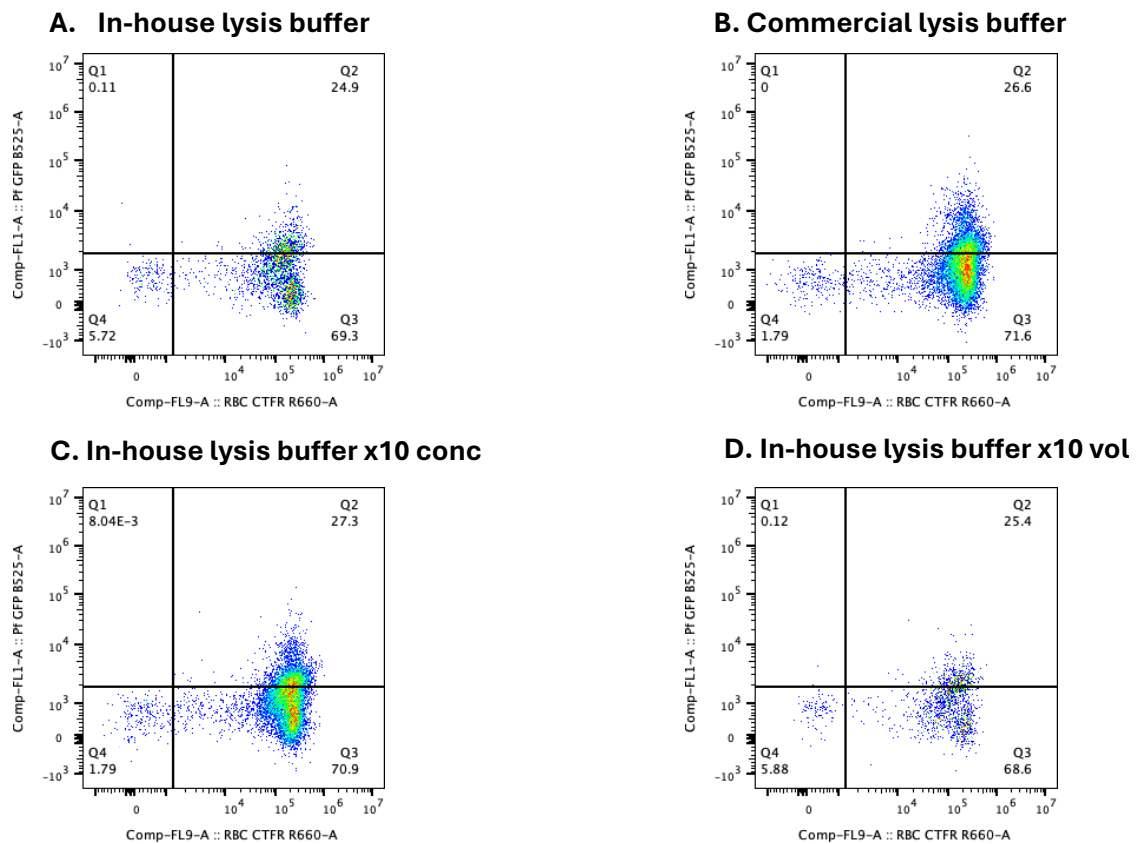

Figure 12. Insufficient lysis of uRBCs did not appear to explain the population of GFP-CellTrace+ monocytes.
Cells are pregated on monocytes. Various lysis buffers were tested to compare populations of GFP-CellTrace+ monocytes, between iRBCs using (A) regular in-house RBC lysis, (B) commercial RBC lysis buffer (Roche), (C) x10 concentration of in-house lysis buffer and (D) x10 volume of in-house lysis buffer. Schizonts were added at an MOI of 5 and incubated for four hours at 37ºC. Data was analysed in FlowJo 10.10. Figure is representative of one experiment.

From these series of optimisation steps, we gained some insight into the possible explanation of this population of GFP-CellTrace+ monocytes although further steps must be taken before this assay can be used to indicate specificity of phagocytosis by patient monocytes.

Discussion

Here, we set out to develop an assay which could measure non-opsonic phagocytosis of iRBCs by monocytes from patients with different levels of immunity to malaria. We designed our experiment using isolated schizonts from an *in vitro* culture of *P. falciparum* 3D7 labelled with GFP. We stained the total population of RBCs present with CellTrace to differentiate between uRBC and iRBC uptake. To set up this assay, we used monocytes from healthy non-infected donor PBMCs. Following few further optimisation steps, this assay could be used to test the specificity and efficiency of phagocytosis by monocytes from patients in endemic and non-endemic countries to compare differences between patients with different levels of underlying immunity and to unravel the role of innate memory in semi-immunity to malaria.

While B and T cell memory responses to malaria have been studied extensively, much less is known about the innate immune response to *Plasmodium spp* [13, 17, 20]. Recently however, research interests have shifted more towards the innate immune system and in particular, the development of innate immune memory.

Phagocytosis has recently been demonstrated to be associated with naturally acquired protection from severe disease in individuals exposed to malaria [31, 32, 33, 34]. However, this has primarily been demonstrated via opsonic activity of antibodies induced by adaptive memory responses. Our hypothesis is that in semi-immune patients, non-opsonic phagocytosis of iRBCs is more efficient and/or more specific, compared to uRBCs, than in naïve individuals. This may be a result of trained immunity that is established in the course of possibly multiple previous *Plasmodium spp*. infections. We aimed to develop an assay which could measure the uptake of both iRBCs and uRBCs to later compare phagocytosis by monocytes of patients with different underlying levels of immunity, recruited as part of the 'DEMIT' study. We developed our assay using isolated schizonts from a *P. falciparum* 3D7 culture labelled with GFP. By staining the whole isolated culture with CellTrace dye, it is possible to distinguish between monocytes that have phagocytosed iRBCs (GFP+CellTrace+) and uRBCs (GFP-CellTrace+). This allows us to determine the specificity of phagocytosis.

The 'DEMIT' study is a multi-centre study performed between Charité University Hospital, Berlin recruiting patients as they receive medical care, and CERMEL, in a region of hyper-endemic transmission. Transport of patient material from our partner site in Gabon to Charité is performed frozen and so, we aimed to develop an assay using frozen PBMCs, that could later be used to test

patient material. We tested pan-monocytes from freshly isolated PBMCs and compared them to monocytes from frozen-thawed PBMCs. We found that freezing and thawing did not appear to induce changes to the functional activity of isolated monocytes, and we could measure the phagocytic activity of these monocytes.

We then considered either using full PBMCs or isolated monocytes for the assay. When isolating monocytes from full, thawed PBMCs by magnetic negative selection, we observed relatively high cell losses and low yields, producing monocyte populations between 1.7 and 3.8% of the initial PBMC population. Therefore, we aimed to use full PBMCs with consideration for the limited patient material available (one aliquot containing maximum 5 x 10^6 PBMCs before freezing). In addition, it has been demonstrated that while *P. falciparum* exposure can amplify the inflammatory response in adherent PBMCs, the same response is not always observed using isolated monocytes [27]. As mentioned, Crabtree et al. demonstrated this by seeding full PBMCs in a round-bottomed plate and removing non-adherent cells after one hour [27]. The remaining adherent cells, once exposed to *P. falciparum*, demonstrated hyperproduction of IL-6 and TNF following restimulation with LPS [27]. This training response was not observed in T-cell depleted PBMCs suggesting a role for the presence of lymphocytes in immune training which is responsible for the increased production of pro-inflammatory cytokines [27]. Importantly, it was observed both in published data and in our experiments, that while longer resting periods induced a reduction in the proportion of CD3+CD19+ cells in the adherent population, some lymphocytes remained [35]. The role that these lymphocytes play in uptake of RBCs by monocytes should be considered. To optimise the population of monocytes during the seeding of PBMCs, we could utilise a plate with larger surface area, such as a flat-bottom plate, to increase the proportion of adherent monocytes relative to remaining lymphocytes present.

Monocyte subsets are determined by their expression of CD14 (co-receptor for toll-like receptor (TLR) 4) and CD16 (FcγRIIIa) and are divided into classical (CD14$^+$CD16$^-$), non-classical (CD14^{dim}CD16$^+$) and intermediate (CD14$^+$CD16$^+$) subclasses [18]. So far, we have only analysed pan-monocytes, including all three populations in our assay. It has been recently debated in literature, what subclasses are most significantly involved in immune responses to malaria and specifically demonstrate enhanced phagocytic responses following previous malaria infection [36, 37, 38, 39]. It is important to note that most published data on this refers to opsonic phagocytosis, and whether these findings are relevant to subclasses in non-opsonic phagocytosis is to be assessed. Zhou et al. demonstrated, in whole blood, increased activity of intermediate monocytes compared to classical monocytes by measuring uptake of ethidium bromide, used to label infected erythrocytes, via opsonic phagocytosis [38]. Notably, without opsonisation,

differences between intermediate and classical monocytes were not significant. It was also shown by Vianou et al., in a cohort of paediatric patients either with cerebral or uncomplicated malaria, that the activity of non-classical monocytes was greater than other subsets in both opsonic and non-opsonic phagocytosis [39]. Our assay has been developed and tested using malaria-naïve PBMCs which will not demonstrate changes that occur due to trained immunity and so limited insight can be gained by assessing monocyte subtypes so far. Most recent data indicate the role of both non-classical and intermediate monocytes although the naturally occurring proportions of each subclass should be considered, particularly when comparing *in vitro* findings to patient data. Classical monocytes typically comprise approximately 85% of a human monocyte population, and so the population size should be taken into account when considering relative contribution of each subtype to the overall phagocytic activity of monocytes [40]. Current research performed in our group, will shortly provide more insight into the *in vivo* relevance of these populations in malaria patients. Using our assay, we will compare non-opsonic phagocytosis of the different monocyte subsets in a larger patient cohort, as data on this is so far very limited.

We found that our results often produced large populations of GFP-CellTrace+ monocytes and trialled several optimisation steps to understand what cells this population is comprised of. We first hypothesised that this population consisted of monocytes that have taken up uRBCs, However, considering that the added isolated schizont populations consisted of approximately 70% schizont-iRBCs and 30% uRBCs, the presence of such a high proportion of monocytes that phagocytosed uRBCs (48.9-76.5% total monocytes) compared to those that phagocytosed iRBCs (9.25-26.6% total monocytes) would be unexpected, regardless of the monocyte's specificity. Therefore, we had to consider other explanations for this population in this frequency.

We cultured uRBCs in the same culture conditions as *P. falciparum* to determine whether changes occur over time or as result of culture conditions, making the uRBCs more susceptible to phagocytosis by monocytes. This may be a result of changes that occur over time like RBC ageing, alterations to the gaseous environment inducing hypoxic conditions, or fluctuations in the media content of essential components required for growth [28, 30]. Aged RBCs have been demonstrated *in vivo*, to undergo rapid phagocytosis by macrophages [28]. Gottlieb at al. physiologically aged RBCs using a hyper-transfusion procedure in mice where erythropoiesis is inhibited [28]. These authors measure senescence by multiple parameters including externalised phosphatidylserine and levels of reactive oxygen species. They demonstrate increased

phagocytosis of senescent RBCs by macrophages in hyper-transfused mice compared to wild-type [28]. We did not observe changes in phagocytosis of 'cultured' RBCs compared to fresh RBCs indicating that our culturing conditions do not appear to induce changes responsible for increasing monocyte phagocytosis of uRBCs. Further testing of the culture media should be performed, in iRBC and uRBC cultures, to determine whether components such as glucose are rapidly consumed by iRBCs, leaving uRBCs deficient of important constituents. In addition, we could confirm the atmospheric make-up using the candle-jar method by culturing in incubators with set gaseous conditions, to outline any differences in RBC phagocytosis.

We then investigated whether the RBC lysis step performed in our assay was sufficiently lysing RBCs that were not phagocytosed by monocytes. By testing the RBC lysis buffer produced in-house at higher concentrations and volume, compared to a commercially available RBC lysis buffer, we found little differences in the population of GFP-CellTrace+ monocytes. To further confirm that these findings indicate sufficient lysis, an experiment could be performed including and excluding the RBC lysis step to assess whether changes are observed in the GFP-CellTrace+ population. This experiment may also indicate whether the population of lysed RBCs is primarily composed of iRBCs or uRBCs.

To test whether uRBCs adhere to the monocyte surface, we performed the co-incubation of RBCs and monocytes at 4°C which should inhibit phagocytosis. What we observed is that also at 4°C a proportion, approximately 20% of monocytes, were GFP-CellTrace+. Still, this frequency was lower than what we observed with incubation at 37°C, when phagocytosis takes place. It appeared that phagocytosis was indeed inhibited, as we did not observe any GFP+CellTrace+ monocytes, as in previous experiments. These results indicate that indeed possibly a fraction of the GFP-CellTrace+ monocyte population might be caused by adherence of RBCs to monocytes. To verify these results, another strategy should be used to inhibit phagocytosis, for example using cytochalasin D, preventing actin polymerisation [41]. Should these findings indicate a similar result, likely this proportion of approximately 20% GFP-CellTrace+ events, are RBCs are adhering to the surface of monocytes and an additional washing step could be added, using PBS and EDTA to prevent this from occurring. Given that we did not observe a population of GFP+ monocytes, if this population has formed as result of adherence, it would appear that all adherent RBCs are uRBCs. Unless uRBCs demonstrate some specificity in this adherence, it's likely that these results could imply an alternative explanation to this population.

We considered that leakage of CellTrace dye, which may occur during or after staining, could be responsible for a portion of the GFP-CellTrace+ population. However, using trans-well plates to test for leakage of the CellTrace stain from RBCs did not clearly demonstrate an explanation to the GFP-CellTrace+ population. By adding PBMCs to the bottom section of the plate and isolated CellTrace-labelled schizonts to the top insert, direct contact between the two cell types is prohibited. Following the phagocytosis incubation, the top inserts were removed, and the cells were stained as normal. Notably, the RBC lysis step that is usually performed was not included as the top insert containing the RBCs was immediately removed after co-incubation. It is possible, that the leakage predominantly occurs after lysing the RBCs during the RBC lysis step as the dye present inside the RBCs might then be released into the media, resulting in CellTrace+ monocytes. Repeating the trans-well experiment with our normal lysis step might give us an insight into this problem. In addition, performing the regular phagocytosis assay with and without the lysis step, should be tested to indicate whether lysis of stained RBCs may contribute to the leakage of CellTrace dye, leading to uptake of the stain by monocytes, contributing to the GFP-CellTrace+ monocyte population. During the development of the standard assay, we added a step which aimed to prevent leakage directly after staining, incorporating a short incubation of CellTrace stained RBCs with culture media to quench excess staining [42]. This could also be added following lysis and could further circumvent the excess stain being taken up by monocytes. As we did observe differences in the proportion of GFP+CellTrace+ population when staining with CTV compared to CTFR, alternative staining could be considered, particularly if leakage also plays a role. A stain which is specific to RBCs, rather than binding to a more general cell structure such as the cytoplasm by CellTrace, might prevent this increased monocyte signal.

To confidently identify the cells which comprise the population of GFP-CellTrace+ monocytes, our assay could be optimised for use with imaging flow cytometry, allowing us to visualise each event and confirm that our staining strategy correctly identifies phagocytosed iRBCs.

A further hypothesis for the origin of the GFP-CellTrace+ population is that the GFP signal of the isolated schizonts is lost over time.

We considered first, the consistency of the GFP expression in our labelled strain. This strain was gifted as part of an academic collaboration and the exact location of the GFP label within the genome is unknown. Selecting for the labelled strain is important during culturing of *P. falciparum* to prevent the replication of the wildtype parasite. We observed by visualising the culture under fluorescent microscopy, that there appeared to be slight inconsistencies to the GFP fluorescence, even if the culture is synchronised and all parasites are at the same

stage (Supplemental Fig. 2). We therefore cultured the labelled strain in cRPMI supplemented with WR, an anti-malarial protein of the phenanthrene class, which has been used previously in the resistance-cassette of transfected *Plasmodium spp*. strains [43, 44, 45]. Treatment of the culture with WR selects for the transfected strain and kills any wildtype strain present in the culture. We found that treatment of our strain with WR appeared not to kill the parasite, and the culture continued to grow. Fluorescence of GFP from cultures using WR-supplemented cRPMI showed some increase (Supplemental Fig. 3) relative to cRPMI-only cultures, and further testing will be performed including a PCR to confirm the insertion of the WR-resistance cassette. However, taking these considerations into account, we performed compensation before each experiment where we saw that GFP signal of isolated schizonts closely correlated to the calculated purity of the schizont isolation (Supplemental Fig. 4). This could indicate that GFP labelling is, infact, consistent although the location of GFP insertion should be confirmed, nonetheless.

Another possible explanation for the loss of GFP signal is its sensitivity to pH [46]. During phagocytosis, phagocytes induce rearrangement of the actin cytoskeleton after the engagement of receptors, such as CD36 [47]. This triggers the formation of small pseudopods around the target particle, or in this case iRBC, which eventually forms the phagosome [48]. During this maturation phase, fusion between other intracellular vesicles and the lysosome gradually reduces the pH as the phagolysosome eventually becomes highly acidic (pH as low as 4.5) [47]. It has been demonstrated that lower pH values (pH < 6) can influence the stability of GFP fluorescence and therefore its detection by flow cytometry [46, 49]. This means, the population of GFP-CTFR+ could also contain formerly GFP+ iRBCs. One possible experiment that could be used to test whether acidification is diminishing the GFP signal, could be to include an inhibitor of lysosome acidification although whether this in turn would impact phagocytosis itself should be carefully considered.

In addition, we considered whether the formation of extracellular vesicles (EVs) may play a role in the uptake of uRBCs. Once *P. falciparum* has invaded RBCs, parasites feed on hemoglobin, producing the waste product hemozoin. Hemozoin is stored inside digestive vesicles which can be released into circulation [50, 51, 52]. EVs, which can be released by many different cells including RBCs and monocytes, have been studied in malaria [52]. *P. falciparum* appears to produce more EVs relative to other *Plasmodium* strains also observed in higher numbers from iRBCs than uRBCs [53, 54]. Perhaps EV release by RBCs could occur over the

course of our experiment, causing vesicles containing hemozoin to adhere to other iRBC and importantly uRBCs and potentially trigger phagocytosis. This possibility, alongside exosome formation, may be factors to take into account, when identifying the population of GFP-CellTrace+ monocytes. However, we must consider that if EV formation occurs, they must be binding preferentially to uRBCs, if they are to explain the population of GFP-CellTrace+ monocytes and whether this is possible remains to be examined. A number of functional changes occur to an RBC once infected, for example, expression of *P. falciparum*-specific proteins as well as structural changes to the RBC surface via phosphatidylserine-induced scramblase activation [55]. If these changes could reduce the adherence of an EV to the surface of an iRBC is to be assessed.

While this study shed light on one method to study non-opsonic phagocytosis of *P. falciparum* iRBCs by monocytes, a number of optimisation steps must be completed before the assay can be used to test patient samples. Additional tests to understand the population of GFP-CellTrace+ monocytes include further investigations into stain leakage, particularly in the context of RBC lysis. Additionally, performing the experiment in a flat-bottom plate may allow us to increase the proportions of monocytes in the adherent cell population, given the greater surface area. In this way, further analysis can also be done using fluorescence microscopy to verify phagocytosis and consistent fluorescent labelling of iRBCs. Finally, optimising this assay for use in imaging flow cytometry would allow us to visualise each event and verify that our strategy allows us to accurately measure non-opsonic phagocytosis to compare iRBC and uRBC uptake.
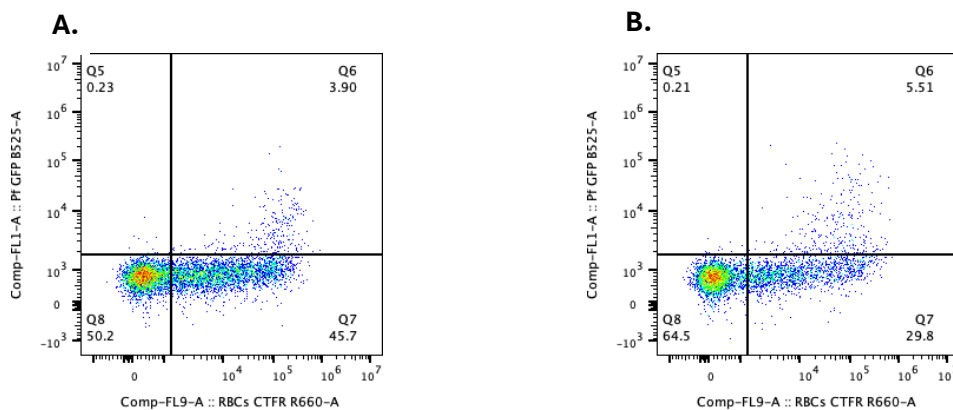
Supplemental Figures
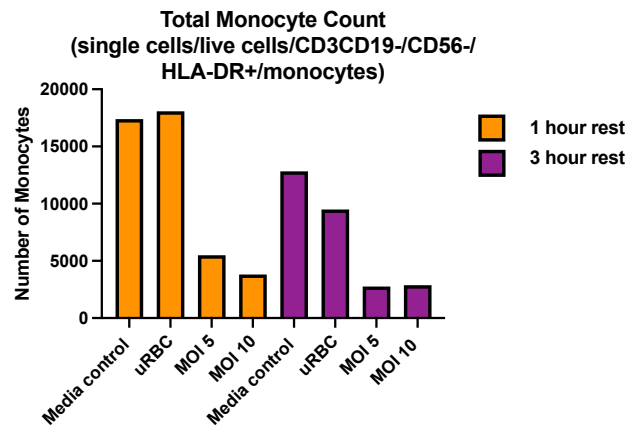
Supplemental Figure 1. Total monocyte counts lower with longer rest periods.
The total number of monocytes recorded by flow cytometry was lower in the media control, uRBC control, MOI 5 and MOI 10, after resting for three hours (in purple) compared to one hour (in orange). Graph produced using GraphPad Prism 10. Figure is representative of one experiment.
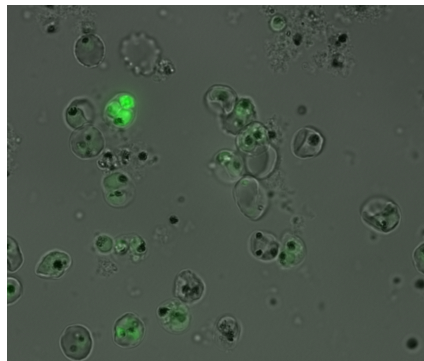

Supplemental Figure 3. GFP expression by synchronised culture was inconsistent.
Approximately 28 hours after culture synchronisation, GFP signal of culture containing primarily trophozoites was measured using fluorescence microscopy with the Echo Revolve microscope visualised using the x100 objective. Parasites, although mostly at equivalent stages, demonstrated inconsistent expression of GFP.

Supplemental Figure 4. GFP expression by schizonts isolated from WR supplemented culture appeared high relative to without WR. *Cells are pregated on monocytes. GFP signal of isolated schizonts (A) maintained in regular cRPMI, showed reduced GFP expression compared to (B) isolated schizonts cultured in WR-supplemented cRPMI. Further testing to confirm this difference is attributable to fluorescence, and not phagocytic differences, is required. Schizonts were added to monocytes at an MOI of 5 and incubated for two hours at 37°C. Samples were measured by flow cytometry and data was analysed in FlowJo 10.10. Figure is representative of one experiment.*
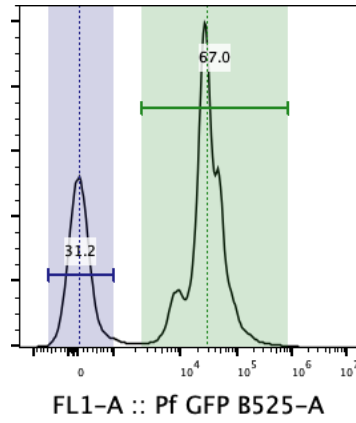
Supplemental Figure 5. GFP single stained compensation.
GFP signal of schizonts isolated using MACS separation performed during compensation, prior to each experiment, clearly demonstrating expression of GFP by schizonts, similar to recorded schizont purity. Data was analysed in FlowJo 10.10. Figure is representative of one experiment.

References

1. Venkatesan, P. The 2023 WHO World malaria report. *The Lancet Microbe* **5**, e214 (2024).

2. Poespoprodjo, J. R., Douglas, N. M., Ansong, D., Kho, S. & Anstey, N. M. Malaria. *The Lancet* **402**, 2328–2345 (2023).

3. Sato, S. Plasmodium—a brief introduction to the parasites causing human malaria and their basic biology. *J Physiol Anthropol* **40**, 1 (2021).

4. Schrum, J. E. *et al.* Plasmodium falciparum induces trained innate immunity. *J Immunol* **200**, 1243–1248 (2018).

5. De Salazar, P. M. *et al.* Severe outcomes of malaria in children under time-varying exposure. *Nat Commun* **15**, 4069 (2024).

6. Bediako, Y. *et al.* Repeated clinical malaria episodes are associated with modification of the immune system in children. *BMC Med* **17**, 60 (2019).

7. Li, J., Liu, L., Chen, D., Yin, W. & Huang, J. Trained immunity from the perspective of Plasmodium infection. *Eur J Immunol* **53**, e2250268 (2023).

8. Ochando, J., Mulder, W. J. M., Madsen, J. C., Netea, M. G. & Duivenvoorden, R. Trained immunity — basic concepts and contributions to immunopathology. *Nat Rev Nephrol* **19**, 23–37 (2023).

9. Bekkering, S., Domínguez-Andrés, J., Joosten, L. A. B., Riksen, N. P. & Netea, M. G. Trained Immunity: Reprogramming Innate Immunity in Health and Disease. *Annu Rev Immunol* **39**, 667–693 (2021).

10. Walk, J. *et al.* Outcomes of controlled human malaria infection after BCG vaccination. *Nat Commun* **10**, 874 (2019).

11. Bekkering, S. *et al.* In Vitro Experimental Model of Trained Innate Immunity in Human Primary Monocytes. *Clin Vaccine Immunol* **23**, 926–933 (2016).

12. Chen, J. *et al.* BCG-induced trained immunity: history, mechanisms and potential applications. *Journal of Translational Medicine* **21**, 106 (2023).

13. Pohl, K. & Cockburn, I. A. Innate immunity to malaria: The good, the bad and the unknown. *Front. Immunol.* **13**, (2022).

14. Herbert Mainero, A., Spence, P. J., Reece, S. E. & Kamiya, T. The impact of innate immunity on malaria parasite infection dynamics in rodent models. *Front. Immunol.* **14**, (2023).

15. Belachew, E. B. Immune Response and Evasion Mechanisms of Plasmodium falciparum Parasites. *J Immunol Res* **2018**, 6529681 (2018).

16. Liehl, P. *et al*. Host-cell sensors for Plasmodium activate innate immunity against liver-stage infection. *Nat Med* **20**, 47–53 (2014).

17. Stevenson, M. M. & Riley, E. M. Innate immunity to malaria. *Nat Rev Immunol* **4**, 169–180 (2004).

18. Xuan, K. M., Bakar, N. A., Fadzli Mustaffa, K. M. & Azlan, M. The role of monocytes in malaria infection. *Cent Eur J Immunol* **48**, 54–62 (2023).

19. Sakoguchi, A. & Arase, H. Mechanisms for Host Immune Evasion Mediated by Plasmodium falciparum-Infected Erythrocyte Surface Antigens. *Front Immunol* **13**, 901864 (2022).

20. Dobbs, K. R., Crabtree, J. N. & Dent, A. E. Innate Immunity to Malaria, The Role of Monocytes. *Immunol Rev* **293**, 8–24 (2020).

21. Walk, J. *et al*. Controlled Human Malaria Infection Induces Long-Term Functional Changes in Monocytes. *Front. Mol. Biosci.* **7**, (2020).

22. Royo, J. *et al*. Changes in monocyte subsets are associated with clinical outcomes in severe malarial anaemia and cerebral malaria. *Sci Rep* **9**, 17545 (2019).

23. Gallo, V., Skorokhod, O. A., Schwarzer, E. & Arese, P. Simultaneous determination of phagocytosis of Plasmodium falciparum-parasitized and non-parasitized red blood cells by flow cytometry. *Malaria Journal* **11**, 428 (2012).

24. Chua, C. L. L., Ng, I. M. J., Yap, B. J. M. & Teo, A. Factors influencing phagocytosis of malaria parasites: the story so far. *Malaria Journal* **20**, 319 (2021).

25. Trager, W. & Jensen, J. B. Human malaria parasites in continuous culture. *Science* **193**, 673–675 (1976).

26. Ulmer, A. J., Scholz, W., Ernst, M., Brandt, E. & Flad, H.-D. Isolation and Subfractionation of Human Peripheral Blood Mononuclear Cells (PBMC) by Density Gradient Centrifugation on Percoll. *Immunobiology* **166**, 238–250 (1984).

27. Crabtree, J. N. *et al*. Lymphocyte crosstalk is required for monocyte-intrinsic trained immunity to Plasmodium falciparum. *J Clin Invest* **132**, e139298.

28. Gottlieb, Y. *et al*. Physiologically aged red blood cells undergo erythrophagocytosis in vivo but not in vitro. *Haematologica* **97**, 994–1002 (2012).

29. Ng, S. *et al*. Hypoxia promotes liver-stage malaria infection in primary human hepatocytes in vitro. *Dis Model Mech* **7**, 215–224 (2014).

30. Crispim, M., Verdaguer, I. B., Silva, S. F. & Katzin, A. M. Suitability of methods for Plasmodium falciparum cultivation in atmospheric air. *Mem. Inst. Oswaldo Cruz* **117**, e210331 (2022).

31. O'Flaherty, K., Roe, M. & Fowkes, F. J. I. The role of naturally acquired antimalarial antibodies in subclinical Plasmodium spp. infection. *J Leukoc Biol* **111**, 1097–1105 (2022).

32. Musasia, F. K. *et al.* Phagocytosis of Plasmodium falciparum ring-stage parasites predicts protection against malaria. *Nat Commun* **13**, 4098 (2022).

33. Chua, C. L. L., Ng, I. M. J., Yap, B. J. M. & Teo, A. Factors influencing phagocytosis of malaria parasites: the story so far. *Malaria Journal* **20**, 319 (2021).

34. Osier, F. H. *et al.* Opsonic phagocytosis of Plasmodium falciparum merozoites: mechanism in human immunity and a correlate of protection against malaria. *BMC Med* **12**, 108 (2014).

35. Nielsen, M. C., Andersen, M. N. & Møller, H. J. Monocyte isolation techniques significantly impact the phenotype of both isolated monocytes and derived macrophages in vitro. *Immunology* **159**, 63–74 (2020).

36. Antonelli, L. R. V. *et al.* The CD14+CD16+ Inflammatory Monocyte Subset Displays Increased Mitochondrial Activity and Effector Function During Acute Plasmodium vivax Malaria. *PLOS Pathogens* **10**, e1004393 (2014).

37. Royo, J. *et al.* Changes in monocyte subsets are associated with clinical outcomes in severe malarial anaemia and cerebral malaria. *Sci Rep* **9**, 17545 (2019).

38. Zhou, J. *et al.* CD14hiCD16+ monocytes phagocytose antibody-opsonised Plasmodium falciparum infected erythrocytes more efficiently than other monocyte subsets, and require CD16 and complement to do so. *BMC Med* **13**, 154 (2015).

39. Vianou, B. *et al.* Monocytes, particularly nonclassical ones, lose their opsonic and nonopsonic phagocytosis capacity during pediatric cerebral malaria. *Front. Immunol.* **15**, (2024).

40. Sherwood, E. R. *et al.* Innate Immune Memory and the Host Response to Infection. *J Immunol* **208**, 785–792 (2022).

41. Schulz, D., Severin, Y., Zanotelli, V. R. T. & Bodenmiller, B. In-Depth Characterization of Monocyte-Derived Macrophages using a Mass Cytometry-Based Phagocytosis Assay. *Sci Rep* **9**, 1925 (2019).

42. Thiam, L. G. *et al.* Feature article: Cell trace far-red is a suitable erythrocyte dye for multi-color Plasmodium falciparum invasion phenotyping assays. *Exp Biol Med (Maywood)* **245**, 11–20 (2020).

43. Witmer, K. *et al.* Analysis of subtelomeric virulence gene families in Plasmodium falciparum by comparative transcriptional profiling. *Mol Microbiol* **84**, 243–259 (2012).

44. Ghorbal, M. *et al.* Genome editing in the human malaria parasite Plasmodium falciparum using the CRISPR-Cas9 system. *Nat Biotechnol* **32**, 819–821 (2014).

45. Mogollon, C. M. *et al.* Rapid Generation of Marker-Free P. falciparum Fluorescent Reporter Lines Using Modified CRISPR/Cas9 Constructs and Selection Protocol. *PLoS One* **11**, e0168362 (2016).

46. Campbell, T. The Effect of pH on Green Fluorescent Protein: a Brief Review. in (2001).

47. Lee, H.-J., Woo, Y., Hahn, T.-W., Jung, Y. M. & Jung, Y.-J. Formation and Maturation of the Phagosome: A Key Mechanism in Innate Immunity against Intracellular Bacterial Infection. *Microorganisms* **8**, 1298 (2020).

48. Underhill, D. M. & Goodridge, H. S. Information processing during phagocytosis. *Nat Rev Immunol* **12**, 492–502 (2012).

49. Mazzola, P. G., Ishii, M., Chau, E., Cholewa, O. & Penna, T. C. V. Stability of Green Fluorescent Protein (GFP) in Chlorine Solutions of Varying pH. *Biotechnology Progress* **22**, 1702–1707 (2006).

50. Olivier, M., Van Den Ham, K., Shio, M. T., Kassa, F. A. & Fougeray, S. Malarial Pigment Hemozoin and the Innate Inflammatory Response. *Front. Immunol.* **5**, (2014).

51. Rathi, A. *et al.* Hemozoin in malaria eradication—from material science, technology to field test. *NPG Asia Mater* **15**, 1–27 (2023).

52. Babatunde, K. A. *et al.* Role of Extracellular Vesicles in Cellular Cross Talk in Malaria. *Front Immunol* **11**, 22 (2020).

53. Vimonpatranon, S. *et al.* Extracellular Vesicles Derived from Early and Late Stage Plasmodium falciparum-Infected Red Blood Cells Contain Invasion-Associated Proteins. *J Clin Med* **11**, 4250 (2022).

54. Kioko, M. *et al.* Extracellular vesicles could be a putative posttranscriptional regulatory mechanism that shapes intracellular RNA levels in Plasmodium falciparum. *Nat Commun* **14**, 6447 (2023).

55. Fraser, M., Matuschewski, K. & Maier, A. G. Of membranes and malaria: phospholipid asymmetry in Plasmodium falciparum-infected red blood cells. *Cell Mol Life Sci* **78**, 4545–4561 (2021).